Bioelectrochemical recovery of silver from wastewater with sustainable power generation and its reuse for biofouling mitigation

Jafar Ali [a, b], Lei Wang*[, a,b], Hassan Waseem [c], Hafiz Muhammad Adeel Sharif [d], Ridha Djellabi [d], Changbo Zhang [e], Gang Pan *[, a,b, f]

[a] *Key Laboratory of Environmental Nanotechnology and Health Effects, Research Center for Eco-environmental Sciences, Chinese Academy of Sciences, 18 Shuangqing Road, Beijing 100085, P. R. China.*

[b] *Research Center for Environmental Material and Pollution Control Technology, University of Chinese Academy of Sciences, Beijing 100049, P. R. China*

[c] *Department of Environmental Engineering, Michigan State University, East Lansing, MI 48823, USA*

[d] *Research Center for Eco-environmental Sciences, Chinese Academy of Sciences, 18 Shuangqing Road, Beijing 100085, P. R. China.*

[e] *Agro-Environmental Protection Institute, Ministry of Agriculture, Tianjin 300191, P. R. China.*

[f] *Centre of Integrated Water-Energy-Food Studies, School of Animal, Rural and Environmental Sciences, Nottingham Trent University, Brackenhurst Campus, Southwell NG25 0QF, United Kingdom*

* Corresponding authors: leiwang@rcees.ac.cn (L. Wang) and gpan@rcees.ac.cn (G. Pan)

Abstract

Precious metals recovery and wastewater treatment using the microbial fuel cell (MFC) is an attractive approach for a sustainable environment. Silver recovery from wastewater and its valorization in the form of silver nanoflakes (AgNFs) brings back waste material to production stream and helps in transition from linear to circular economy. In the present study, bioelectrochemical performance of MFC fed with silver laden artificial wastewater (MFC-Ag)

was compared with MFC fed with potassium ferricyanide (MFC-FC) and MFC fed with phosphate buffer as catholyte (MFC-blank). High silver removal (83 ± 0.7%) and recovery (67.8 ± 1%) efficiencies were achieved from MFC-Ag after 72 h operation. The maximum power density (3006 mW/m^3) and current density (34100 mA/m^3) of MFC-Ag were found to be significantly higher than the MFC-FC and MFC-blank. High chemical oxygen demand (COD) removal efficiency of MFC-Ag (82.7 ± 1.5%) compared with MFC-FC (76 ± 2) highlighted the suitability of silver laden wastewater as a cost effective catholyte. The high coulombic efficiency (8.73 ± 0.9 %) and low solution resistance (24.38 Ω) for MFC-Ag also indicate the potential of silver laden wastewater for large scale applications. Analytical characterizations of electrochemically recovered silver revealed the pure (99%) and crystalline AgNFs with a mean diameter of 18 ± 1.2 nm on the cathode surface. Furthermore, a significant anti-biofouling activity of recovered AgNFs indicate the valorization of waste by current study with potential applications in several industrial and environmental processes. Our method has diverse potential to scale up the MFC technology for industrial waste management as a closed loop process with minimum facilities and higher sustainability.

Keywords: Microbial fuel cell; Resource recovery; Sustainable; Anti-biofouling; Silver; wastewater

1. Introduction

Silver has widely been used in various industries such as jewellery, photography, medical/pharmaceutical applications, personal care products (PCP) and electronic industries (Dutta, 2019; Ho et al., 2018). Silver discharge from different industries can accumulate in the environment can cause serious clinical implications owing to its potential toxicity (Lei et al., 2018). The United States Environmental Protection Agency (US-EPA) has recommended 0.1 and 0.01 mg Ag per litre of water as permissible limits for human beings and aquatic

invertebrates respectively (Greulich et al., 2012; Kahlon et al., 2018). Also, European Union has listed the silver as a priority pollutant for the aquatic environment (Directive 2006/11/EC) due to increased demand of silver-based products in Europe, North America, and Asia (Deycard et al., 2017). Presence of silver ions and silver nanoparticles (AgNPs) can lower the efficiency of biological wastewater treatment plants(Ward et al., 2019). Recently, a four percent increase in the global industrial demand and a two percent fall in mining supply of silver has been reported (Deycard et al., 2017; Dutta, 2019). A gap of 6000 tons between production and usage of silver is continuously growing annually during the last decade (Grandell and Thorenz, 2014). Hence, silver recovery from wastewater and secondary sources would not only be an eco-friendly process but would also be helpful in fulfilling the global demand of the expensive metal. Currently, numerous technologies are being used for the extraction and recovery of silver from the waste and wastewater, which include bio-sorption, bio-hydrometallurgical, leaching, ion exchange adsorption, reverse osmosis, ultrafiltration, cementation and electrochemical deposition (Choi and Cui, 2012; Syed, 2016).

Sorption and desorption decrease the bioavailability of silver in aqueous solutions (Staroń et al., 2017). Hybrid cyanidation and high-pressure membrane processes have been employed to recover silver from mining wastewater (Koseoglu and Kitis, 2009; Lei et al., 2018). Besides, industries have adapted various hydrometallurgical processes integrated with pyrolysis to recover precious metals from the waste printed circuit boards (Niu et al., 2017; Rigoldi et al., 2018). Unfortunately, hydrometallurgical processes are based on dissolving noble metals by acids and caustic leachates, which is not a cost effective process. Several other technologies, like cementation, may involve the use of toxic thiocyanate and subsequent production of secondary pollutants may limit their applications on a larger scale (Rigoldi et al., 2018). Thus, more efficient and eco-friendly strategies must be developed for sustainable silver recovery from the wastewater. Microbial fuel cell (MFC) technology has emerged as a promising way

to recover precious metals, harvest electrical energy and wastewater treatment through microbial metabolism (Ali et al., 2018; Liu et al., 2005).

Despite the significant improvements in its performance and design, MFC technology is still far from practical applications due to relatively higher costs, slow reaction kinetics, low power density and high internal resistance. Terminal electron acceptor (TEA) in the cathodic chamber plays a crucial role in modulating the performance of MFC. Molecular oxygen, ferricyanide, and permanganate are among the most commonly used TEAs due to high redox potential and low overpotential. However, slow reaction kinetics for oxygen reduction reaction (ORR) and frequent replacement of precious catholytes are practically unsustainable (Liu et al., 2005). Metal ions with high redox potential such as Cr^{6+}, Cu^{2+}, Ag^{+}, Hg^{2+} can be reduced to stable metal nanostructures on the cathode, which exemplify the ability of MFC to generate electricity with metal recovery from wastewater (Nancharaiah et al., 2016). Majority of studies have reported the reduction of hexavalent chromium in MFC, which might be due to its high redox potential. Cathodic reduction of copper (Cu) in dual chamber MFC was done from $CuSO_4$ solution in 288 h (Heijne et al., 2010). Retrieval of three precious metals (Au, Cu, Ag) with electricity generation by coupled redox reactor was also studied (Zhang, H.-M. et al., 2017). A three dimensional MFC recovered the cobalt from striping solution of the spent lithium-ion batteries with low power production (Huang, T. et al., 2019).

Silver has high standard redox potential [Ag^{+}/Ag^{0}, E^{0} = 0.799 V (vs. SHE)], and it can serve as a potential TEA which will lead to silver recovery coupled with wastewater treatment and electricity production. Choi and Cui (2012) provided the earliest demonstration of the silver recovery with a power density of 4.25 W/m^2 in an MFC used for jewellery wastewater treatment. Similarly, ammonia chelated silver alkaline wastewater was used to recover 1.6 g of silver and 3.2 J of energy in BES (Wang et al., 2013). Effect of various operational parameters on silver recovery and performance of BES were evaluated (Ho, N. et al., 2017; Ho, N.A.D. et

al., 2017). A bioelectrochemical system (BES) recovered the silver from wastewater containing diamine complex while power production was enhanced with the addition of 10 mM $NaNO_3$ as a supporting catholyte (Ho et al., 2018). However, aforementioned studies have some drawbacks such as the very high concentration of the silver, i.e., 1000-3000 mg/L was used. Though real wastewater may not contain such a high concentration of silver, thus negating the MFC applications for silver recovery from real wastewater. Also, addition of supporting catholytes to enhance power density is not a sustainable approach (Ho et al., 2018). High internal resistance due to anion exchange membranes, substrate loss from the anode and Ag^+ ions toxicity for biofilm also contributed for low efficiency (Ho, N. et al., 2017). Moreover, the valorization of silver waste through MFCs needs to be explored, which can help in moving towards the circular economy. For example, AgNPs are already known for their anti-biofouling properties (Yang et al., 2018). So, silver recovered from wastewater could serve as a cheap antibiofouling materials along with catalytic properties. Pure cultures are considered more suitable to explore the microbe-electrode interactions, required to scale up the bioelectrochemical recovery of precious metals (Nimje et al., 2012).

In fact, silver recovery from the wastewater using MFC is still in its infancy, hence detailed understanding about the silver recovery from wastewater using MFC and re-utilization of recovered metals is highly needed to apply this lucrative technology for real wastewater. Thus, the aim of the current study was to present an alternative approach for silver recovery from wastewater with bioenergy generation using MFC from low concentrated wastewater and valorization of silver waste for anti-biofouling applications. Compared with other studies our method has provided a one-step resource recovery and its valorization for environmental applications along with bioenergy production as a closed loop, and it has diverse potential to scale up the MFC technology for industrial wastewater with minimum facilities and high sustainability.

2. Materials and methods

2.1. Anodic inoculum, electrolytes preparation

The pure culture of *Pseudomonas aeruginosa* (MK 163529) was obtained from the key laboratory of environmental nanotechnology and health effects, RCEES, Beijing, China. It was then suspended in LB broth to propagate it further. *Pseudomonas aeruginosa* culture was serially diluted in phosphate buffer to get 1-5 × 10^7 cells/mL. Furthermore, annolyte was prepared by dissolving the (g/L) 1.0 $C_2H_3NaO_2$, 4.4 KH_2PO_4, 3.4 K_2HPO_4, 1.0 KNO_3, 0.5 NaCl, 0.2 $MgSO_4$, $CaCl_2$ 0.014 and 1 mL of trace elements solution [dissolving the (mg/L) 0.39 $Na_2MoO_4{\cdot}2H_2O$, 0.22 $ZnSO_4{\cdot}7H_2O$, 1.81 $MnCl_2{\cdot}4H_2O$, 0.08 $CuSO_4{\cdot}5H_2O$ and 2.86 H_3BO_3 in distal water]. Three different catholytes were prepared containing 500 mg/L of $AgNO_3$ in distal water, and 500 mg/L of $K_3[Fe(CN)_6]$ in 100 mM phosphate buffer and only 100 mM phosphate buffer.

2.2. MFC construction and operation

Three identical dual chamber microbial fuel cells [classification based on catholytes: MFC-Ag ($AgNO_3$), MFC-FC (Potassium ferricyanide) and MFC-blank (buffer)] made of Plexiglass were used to study the simultaneous silver recovery and electricity generation with wastewater treatment. MFC-Ag was the experimental cell, and MFC-FC & MFC-blank worked as control cells to compare the electrochemical performance. Each chamber had an active working volume of 160 mL. Graphite fibre brush (3.5 cm long and 2.5 cm in diameter) and graphite felt (4 × 2.5 cm) purchased from Shanghai Hesen Electrical Co., Ltd. was used as anode and cathode of MFCs respectively. Pre-treatment of electrodes was done by overnight incubation in acetone solution followed by heating in a muffle furnace at 450 °C about 30 min as described by Cheng et al. (2006). Proton exchange membrane (PEM, Nafion™ 117, Dupont Co.) with an active surface area 12.56 cm^2 was used as a separator between anode and cathode chambers. However, pre-treatment of PEM was done by boiling in H_2O_2 (30% v/v), deionized water,

H_2SO_4 (0.5 M), and then stored in deionized water, each for one hr as described in the literature (Sravan et al., 2017).

The distance between two electrodes was 4 cm, and titanium wire was used to connect the electrodes and external resistance (Fig. 1). After successful installation of MFCs, each anode chamber was fed with same anolyte and *Pseudomonas aeruginosa* to develop a biofilm. While the catholyte was different in each MFC as described in section 2.1. Nitrogen purging was performed to remove the dissolved oxygen (DO) from each chamber. Initially, MFCs was allowed to run in open circuit mode at room temperature. When a stable open circuit potential (OCP) was achieved, the MFCs were ready for electrochemical analysis. A 1 KΩ resistance was connected externally to measure the voltage generation (Fig. 1). Anolyte and catholyte were replaced from time to time when OCP was below the 0.25 mV.

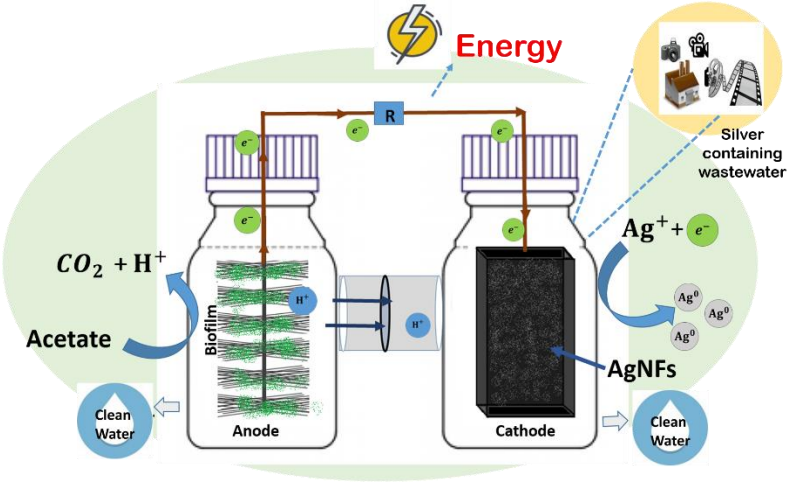

Fig. 1. Schematic illustration of MFC describing the working principal and components

2.3. Analytical methods and calculations

2.3.1. Electrochemical characterization of MFC

All MFCs were operated with different catholytes to compare the electrochemical performance of MFC-Ag coupled with recovery of silver nanoflakes (AgNFs). Cell voltage was continuously recorded for every 20 min using a multimeter data acquisition system (model

2700 Keithley Instruments, Cleveland, USA). Polarization curves were drawn by linear sweep voltammetry (LSV) performed in two electrode mode, where anode was working electrode and cathode served as a counter as well as a reference electrode. The potential was scanned from open circuit potential (OCP, vs. cathode) to 0 V at the scan rate of 1 mVs^{-1} in the reverse direction. Current (I) and Power (P) were calculated using voltage data and the ohms law as ($V = IR_{ext}$) or Power ($P_{max} = V \times I$). The power density was computed by normalizing the power with anodic working volume. Electrochemical impedance spectroscopy (EIS) measurement was done over a frequency range from 100 kHz to 10 mHz with an AC signal of 10 mV amplitude at OCP using the potentiostat CHI660A system (CH Instruments, Inc.) in two electrode mode.

Electrochemical performance of MFCs was also investigated by Tafel analysis using the potentiostat CHI660A system (CH Instruments, Inc.) in three electrode mode. Anode and cathode served as working and counter electrode respectively with Ag/AgCl as a reference electrode. This technique is useful to study the electrochemical reaction kinetics and mechanism of electrode reactions involved in biofilms. Tafel equation describes the relationship between the electrode overpotential and the current density in the high overpotential region and can be expressed as equation (3). In equation.3 η is the overpotential (vs. Ag/AgCl) against which current density (i) is measured, F the Faraday constant (96, 485 C/mole), R the ideal gas constant (8.31 J/mol K), T the temperature (K) and β the symmetry factor (a critical constant reflecting the activation energy).

Moreover, i_0 is exchanged current density obtained from extrapolation of the linear region of the Tafel plot. However, CV analysis was carried out in a conventional three-electrode cell using CHI660A system (CH Instruments, Inc.). The anode of MFCs was used as the working electrode, and Ag/AgCl as a reference electrode, while the cathode served as the counter electrode. The potentials were applied from − 0.8 V to + 0.8 V (vs. Ag/AgCl) at a scan rate of

10 mV/s with continuous monitoring of the current response. The CV was also performed after anolyte replacement in all anodes and spent removed from the anode of all MFCs to explore the main electron transfer mechanism involved in anodic biofilm (Ndayisenga et al., 2018).

$$ln(i|i_{\circ}) = \frac{\beta F\,\eta}{RT} \qquad (3)$$

2.3.2. COD removal and columbic efficiency

To analyse the COD removal efficiency of anodic biofilm during the complete cycle of MFCs. Sample aliquots were taken from anolyte at frequent intervals of 12 h. Before analysis samples were filtered through syringe filter PTFE 0.45 µm (advanced Japan), COD was measured using the COD meter and high range (0-1500 mg/L) kit (Dr 2800, HACH, Loveland, CO, USA). Finally Coulombic efficiencies (CE) were calculated according to the Cheng et al. (2006), where, M is the molecular weight of oxygen, I is current, F is Faraday constant, n is the number of electrons required for reduction of 1 mole of oxygen, V is the working volume of anodic chamber ΔCOD is the difference between initial and final COD after time.

$$CE = \frac{M\int_0^t Idt}{FnV\,\Delta COD} \qquad (4)$$

2.3.3. Silver removal and Silver recovery efficiency

Samples from catholyte of MFC-Ag were taken after 72 h, and Ag^+ ions concentration was measured by Inductively Coupled Plasma-optical emission spectroscopy (ICP-OES Agilent 7500 series, Japan). The silver removal efficiency was calculated using equation 5. Where C_0 is the initial Ag^+ concentration in the catholyte (mg/L), C_t is the remaining Ag^+ concentration in the catholyte at time t (mg/L). However, silver recovery efficiency was estimated from the mass of AgNFs deposited (M_d) on the electrode vs. removed concentration from the catholyte and equation. 6.

$$\text{Silver removal efficiency (\%)} = E_{Rem} = \frac{C_0 - C_t}{C_0} \times 100 \qquad (5)$$

$$\text{Silver recovered efficiency}\,(\%) = E_{Rec} = \frac{M_d}{C_0 - C_t} \times 100 \quad (6)$$

2.4. Characterization of recovered silver nanoflakes

After completion of 72 h successful operation of MFCs, the cathode from MFC-Ag was carefully removed to characterize the deposited AgNFs on its surface. X-ray diffraction analysis of the cathode was performed using X-ray diffraction machine (XRD, PANalytical Empyrean, diffractometer equipped with a Cu Kα1 radiation). Surface morphology and elemental composition of deposited silver nanoflakes were characterized by scanning electron microscopy (SEM, S4800, HITACHI), energy dispersive X-ray spectroscopy (EDX, Horiba) and X-ray fluorescence (ARL-PERFORM'X SEQUENTIAL XRF, USA). The X-ray photoelectron spectroscopy (XPS, ESCALAB 250) was performed to analyse the elemental composition and chemical state on the surface of graphite felt cathode and data was collected at an axis ultra-ESCA system with monochromatic Al Kα standard radiation source. Furthermore, AgNFs were scrapped from the graphite electrode to explore the detailed morphology of AgNFs by HRTEM (JEM 2100-plus transmission electron microscope, JEOL, Tokyo, Japan) operated at an accelerating voltage of 200 kV.

2.5. Evaluating the antifouling potential of the silver deposited electrode

2.5.1. Agar diffusion and broth dilution method

The anti-biofouling activity of the electrochemically deposited AgNFs on graphite felt was evaluated by the agar diffusion method. *Pseudomonas aeruginosa*, *Shewanella putrefaciens*, and *E.coli* were selected as model strains to investigate the anti-biofouling potential of in situ modified cathode. First of all, bacterial cultures were inoculated in sterilized nutrient broth (pH 7.4 ± 0.2) and incubated in shaking incubator (160 rpm.) at 37 ˚C for 24 h. Subsequently, the bacterial suspension was diluted by 1-5 × 10^7 cells/mL with NB. A total of 20 µL from each diluted bacterial solution was well spread on two different nutrient agar to

make a lawn. Silver-deposited electrode (Ag-electrode) from MFC-Ag and control (without silver) were cut into circular pieces with 2.5 cm in diameter. Later on, these pieces of Ag-electrode and control were placed on the freshly prepared lawns of bacteria. After overnight incubation at 37 ˚C, the inhibition zones were measured to calculate the anti-biofouling activity. A correlation between anti-biofouling activities and recovered silver was obtained by modified broth dilution method. In situ modified cathode pieces (2.5 cm) from MFC-50, MFC-100, MFC-150, MFC-250, and MFC-500 were dispensed in five test tubes containing 10 mL of Mueller Hinton broth. An unmodified cathode was used as a control with the same treatment. Then *E. coli* dilution (500 µL) prepared in the same medium and adjusted to 0.5 McFarland scale was inoculated in all test tubes and incubated at 37 ˚C for 12 hours. And growth was measured at 600 nm using a spectrophotometer.

2.5.2. Activated sludge immersion test

Furthermore, anti-biofouling potential of the Ag-electrode was also evaluated by sludge immersion test. The Ag-electrode and control were immersed in activated sludge to observe the biofilm formation up to 10 weeks. Biofilm formation on the electrode samples was observed by SEM (S4800, HITACHI) and confocal laser scanning microscope (CLSM, Zeiss LSM 510 META, Carl Zeiss, Germany) equipped with a plan-apochromat. For the sample preparation electrodes were cut from the centre of the intensively biofouled area, then live, and dead cells were stained using the red fluorescent propidium iodide (PI) and 4′,6-diamidino-2-phenylindole (DAPI Sigma, Germany). Finally, images were obtained using a 63 × objective lens with a 0.95 numerical aperture. A 543 nm helium/neon laser was used to excite the propidium iodide-stained cells. Simulated three-dimensional images were generated by the use of IMARIS software (Bitplane, Switzerland).

3. Results and Discussion

265 *3.1. Open circuit potential and polarization curves*

266 The open circuit potentials (OCP) of three MFCs (MFC-Ag, MFC-FC & MFC-blank)
267 were gradually increased and reached the stabilized OCP as 0.70 V, 0.68 V, and 0.65 V after
268 36 h, 40 h and 44 h of operation respectively. Although no remarkable difference in final OCP
269 values of all MFCs was observed, but the time to achieve this OCP was significantly lesser for
270 MFC-Ag among the others. Different upsurge rates of OCP in MFCs can be linked with the
271 availability of different TEAs (Srikanth and Mohan, 2012). Polarization curves were plotted
272 by LSV, at the stable phase of operation, to study the maximum power production using silver
273 laden wastewater compared with conventional catholytes for each MFC.,. Polarization profiles
274 depict that MFC-Ag has delivered the maximum current density of 34100 mA/m^3 which was
275 approximately 1.3 and 1.5 times higher than the current density of MFC-FC (25600 mA/m^3)
276 and MFC-blank (22375 mA/m^3) respectively (Fig. 2a). The maximum power density extracted
277 from MFC-Ag (3006 mW/m^3) was 1.3 times higher than MFC-FC (2310 mW/m^3) and 5.6 times
278 higher than MFC-blank (528 mW/m^3) (Fig. 2b). Polarization curves of MFC-Ag indicated the
279 cell design point (CDP) was ~70 Ω accounting the maximum power density. The low CDP
280 value suggests the feasibility of MFC treating the silver laden wastewater in the order of small
281 applications in LED, rotary discs and monitoring devices in waste management areas (Sravan
282 et al., 2017; Srikanth and Mohan, 2012).

283 The high current density and power density for the MFC-Ag indicate that Ag
284 contaminated wastewater has effectively served as TEA in the cathode to facilitate the
285 simultaneous silver recovery and sustainable power production from wastewater. Availability
286 and type of suitable TEA have a significant influence on the anodic oxidation and electrogenic
287 activity of MFCs (Choi and Cui, 2012; Sravan et al., 2017). The current study has demonstrated
288 a comparable power production to previous studies which have used a high concentration of
289 precious catholytes. For example, Ho, N. et al. (2017) reported the approximately similar power

density (3385 mW/m^3) to current study using the 2000 mg/L of catholyte. In another investigation a power density of 641.84 mW/m^3 was extracted from 1000 mg/L of silver containing catholyte, however power density in present study was 5 times higher (Ho et al., 2018). Effective utilization of industrial wastewater as a cheap catholyte will help to scale up MFC technology avoiding the frequent replacement of expensive TEAs. Our method is expected to reduce industrial waste generation and to improve the environmental sustainability by efficient resource management.

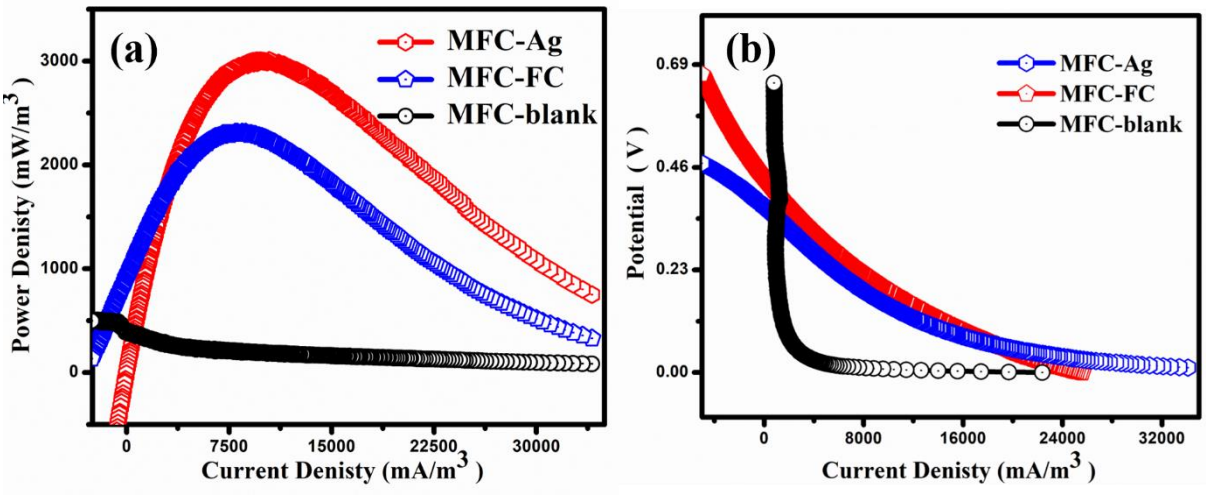

Fig. 2. Polarization curves of MFCs drawn by LSV (a) power densities vs. current density (b) potential of MFCs vs. current density

3.2. Electrochemical impedance spectroscopy and Tafel analysis

Electrochemical impedance spectroscopy (EIS) was performed to measure the internal resistance of all MFCs offered during the electrochemical reactions. Electrolyte resistance, polarization /charge transfer resistance, and diffusion resistance were estimated by Nyquist plot. Electrochemical fitting of impedance spectra was also done to the Randles equivalent circuit using the Zview software. As there was only one semicircle for all MFCs, so one-time constant model (OTCM) was opted to determine all other parameters, where ohmic resistance (R_o) was in series with a parallel combination of capacitance of MFCs (C_{dl}) to the

Warburg/diffusion resistance (W) having charge transfer resistance (R_{ct}) in series. The Nyquist plot of the EIS spectra was measured during the stable phase of the MFCs (Fig. 3a). Reaction kinetics of electrode and electrolyte interface were investigated by fitting the impedance data to the Randles equivalent circuit with the one-time constant model. Fit parameters are also shown in Table 1. Ohmic resistance (R_s) usually contribute to the significant part of the internal resistance of the system, including the sum of total resistance from the biofilm, electrode, and electrolyte. MFC-Ag displayed the lower R_o (24.38 Ω) as compared with MFC-FC (90 Ω) and MFC-blank (108 Ω). The solution resistance (R_s) has a direct influence on maximum power production in MFCs (Islam et al., 2017; Logan et al., 2018). Another critical component of internal resistance is charge transfer/polarization resistance (R_{ct}), which arise from charge transfer barriers, either from electron transfer between capacitive material and current collector or ion transfer between capacitive material and electrolyte. In this study, R_{ct} was of the order of 5.413 Ω, 21.78 Ω, and 23.7 for MFC-Ag, MFC-FC, and MFC-blank, respectively. Warburg element (W) specify the diffusional resistance during the mass transfer toward and away from electrodes. Low polarization resistance (R_{ct} & W) direct the small activation losses, concentration losses and high exchange current density in MFC-Ag as compared with control MFCs as suggested by the Tafel equation (Kim and Chang, 2018; Yong et al., 2014). The overall low internal resistance of MFC-Ag can be linked with significantly improved reaction kinetics. Consequently, silver loaded wastewater has improved the conductivity of catholyte, which will also help in enhanced AgNFs recovery and sustainable power production. The high internal resistance of MFC is considered a major hurdle for the high power density and large scale applications. Previously, various complicated methods have been used to load silver nanomaterials at cathode to reduce internal resistance and to improve the power production in MFCs (Islam et al., 2017; Zhao et al., 2019). In this study, electrodeposition of silver resulted as an additional advantage with wastewater treatment, thereby presenting a facile and clean

method for in situ modification of electrodes. Waste minimization and renewable energy generation intend to improve efficiency of sustainable industrial processes. The bio-electrochemical performance and electrode kinetics of all MFCs were also evaluated through Tafel analysis. This analysis helps to estimate the electrochemical activity of biofilms favoured by different TEAs in MFCs. Tafel slope ($RT/\beta F$) is an indirect measure of electron transfer efficiency among different MFCs fed with different catholyte (Equation .4). The exchange current densities (i_0) were obtained from extrapolating the linear region of Tafel slopes. The calculated exchange current densities (i_0) of MFC-Ag (0.086 Acm^{-2}), MFC-FC (0.084 Acm^{-2}) and MFC-blank (0.05 Acm^{-2}) corresponds to the oxidative Tafel slopes at 4.9 V/dec, 4.8 V/dec and 10.8 V/dec, respectively. High exchange current densities (i_0) and lower Tafel slopes indicate the higher electron transfer efficiencies in MFC-Ag (Fig. 3b). Although Tafel slope for MFC-FC was approximately close to that of MFC-Ag, but higher over-potential will also affect the exchange current and ultimately will hinder the reaction kinetics in the former. Tafel analysis also provides a visual understanding of activation losses during the electrochemical reactions such as ORR and OER (Raghavulu et al., 2012). MFC-blank showed the highest activation losses due to unavailability of any effective TEA in the solution. Comparable Tafel slope values of MFC-Ag and MFC-FC also suggest that silver contaminated water can serve as an alternate and sustainable TEA for MFCs. Enhanced electron transfer efficiency of MFC-Ag will also improve silver recovery and bioenergy generation. Overall simultaneous silver recovery and bioenergy generation from wastewater will be a closed loop process for an industrial economy with no harmful impacts on the environment.

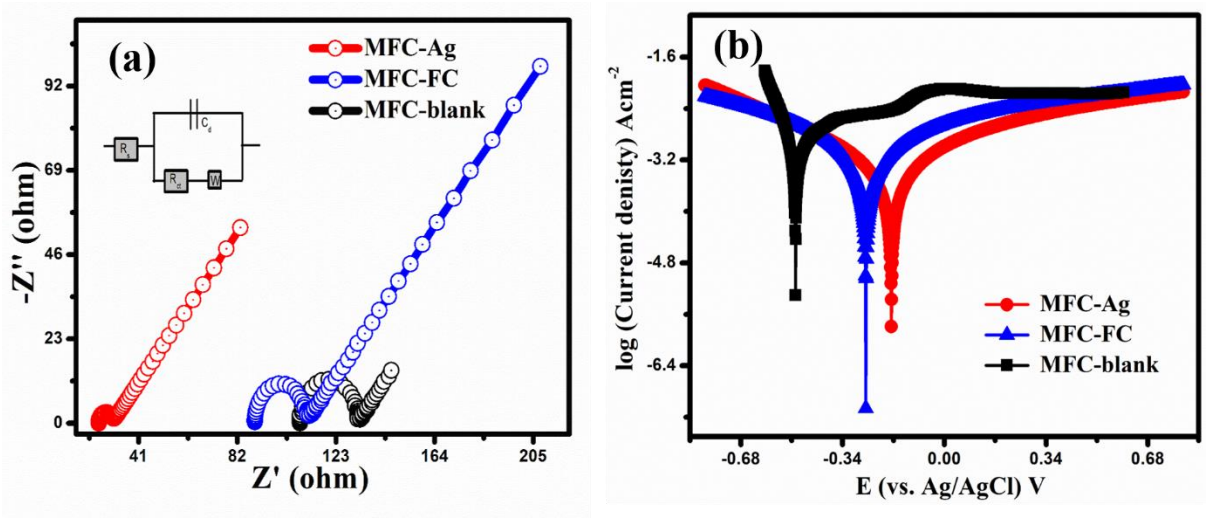

Fig. 3. EIS and Tafel plots (a) electrochemical impedance spectrum of all MFCs showing the internal resistances, (b) Tafel plots describing the activation loses and Tafel slopes

Table. 1. Details of electrochemical impedance spectroscopy results and parameters

Element	MFC-Ag	MFC-FC	MFC-blank
Ohmic resistance	24.38	89.27	108.1
Charge transfer resistance	5.513	21.8	23.76
Capacitance	$5.53E^{-5}$	$2.5E^{-5}$	$5.01E^{-06}$
Warburg element	0.05284	0.19	0.028
Error (%)	0.024	0.012	0.3

3.3. Cyclic Voltammetry

To understand the regulatory effect of silver ions (catholyte) on the anodic biofilm, cyclic voltammetry (CV) analysis was performed during the stabilized phase of MFCs in open circuit mode at the scan rate of 10 mV/s. Cyclic voltammogram from MFC-Ag showed the oxidation and reduction peaks centred around 0.22 V and - 0.37 V (Fig. 4a). While, oxidation-reduction peaks for MFC-FC (0.30 V & 0.44V) and MFC-blank (0.24 & 0.35V) evinced the similar

redox-active molecules in all MFCs, which corresponds to the coenzyme NADH oxidation and cytochrome redox potential of *Pseudomonas aeruginosa* (Fig. 4). These respiratory proteins are essential for electron transfer during the metabolism of bacteria (Feng et al., 2010; Zhang, P. et al., 2017). Numerous studies have reported the exceptional contribution of endogenous mediators such pyocyanin for *Pseudomonas aeruginosa* in various MFCs (Yong et al., 2014). Relatively high oxidative (i_o) = ($2.151e^{-3}$A) and reductive currents (i_r) = $-1.009e^{-3}$A than the MFC-FC (i_o =$4.304e^{-4}$A & i_r = $-8.1209e^{-4}$A) and MFC-blank (i_o =$1.63e^{-4}$A & i_r = $-1.509e^{-3}$A) were observed (Fig. 4). The high oxidative current was ascribed to the low activation losses and efficient electron transfer kinetics as a result of improved oxidation of acetate (Sravan et al., 2017). The CV results are also in agreement with the outcomes of EIS and Tafel plots.

To explore the underlying electron transfer mechanism in all MFCs, a CV analysis was carried out after anodic media replacement and spent solution. Cyclic voltammogram further aided the understanding of the electron transfer kinetics and metabolic changes in terms of redox mediators and substrate degradation efficiency (Grobbler et al., 2018). Rapid retrieval of voltage and CV analysis showed the direct electron transfer mechanism was dominant for all the MFCs (Fig. 4). Moreover, extracellular mediators like phenazines were not detected in CV analysis, which might be membrane-bounded redox active moieties (Saunders and Newman, 2018). However, the reductive currents can be correlated with the reduction of Ag ions, which implies that silver containing wastewater will lower the cost of catholytes and improve the overall efficiency required for large scale applications of MFC. Therefore, our method may provide a sustainable approach for on-site waste management and resource recovery from electronic industrial wastes.

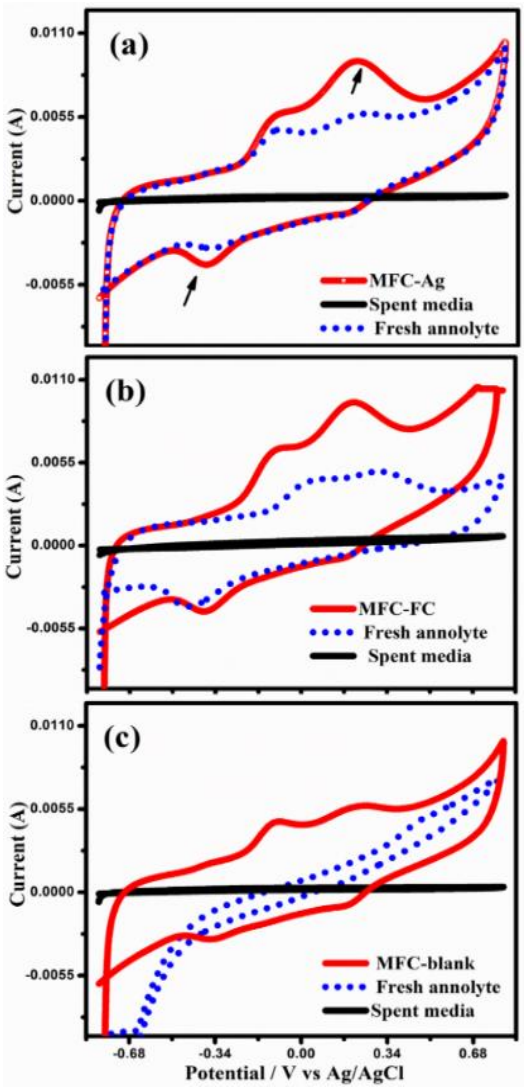

389

390 Fig. 4. Cyclic voltammogram of MFCs (a) MFC-Ag, (b) MFC-FC and (c) MFC-blank

391

392 *3.4. Simultaneous wastewater treatment, silver removal, and electricity generation*

393 After the electrochemical characterization, all MFCs were connected with 1kΩ resistance
394 for evaluating the electricity generation and wastewater treatment in the presence of different
395 catholytes, where acetate served as an electron donor. Electricity generation profile indicates
396 that MFC-Ag produced a relatively stable voltage as compared with control MFCs (Fig. 5a)
397 Although initial overpotential was low in MFC-FC, the voltage was dropped sharply after 30
398 h operation, which can be ascribed with the unavailability of TEA. Periodic COD removal

efficiency profile indicate that TEA replacement in MFC-FC could upsurge and stabilize the voltage generation, thus hampers the large scale applications of MFC. Similarly, MFC-Ag showed the highest COD removal efficiency (82.7 ± 1.5%) and coulmbic efficiency (8.73 ± 0.9%) as compared with MFC-FC (COD: 76 ± 2.1%, CE: 2.73 ± 0.2%) and MFC-blank (COD: 52.2 ± 1.2%, CE: 1.6 ± 0.13%) respectively (Fig. 5b). This COD removal efficiency was higher than previous studies reporting the bioelectrochemical recovery of silver (Ho et al., 2018; Wang et al., 2013). The highest COD removal efficiency of MFC-Ag corroborate the availability of TEA and enhanced electrogenic activities of anodic microbes (Sravan et al., 2017; Zhang et al., 2015). In the past, most of the MFCs studies had majorly focused power production instead of COD removal. Although coulmbic efficiency is sufficient to explain the amount of current production, but COD removal efficiency is a crucial parameter to analyse the treatment effciency of wastewater treatment reactors and it must be low to meet discharge limitations (Zhang et al., 2015). Therefore, high COD removal efficency is beneficial for enhanced electrogenic activity and sustainable resource recovery from indutrial wastewater (Djellabi et al., 2019). Simultanous wastewater treatment and enhnaced power production using MFC also highlighted the feasibility to sacle up MFC technology. Integration of MFC with other waste management processes at industries will reduce energy consumption and lower the carbon foot print. Current method of silver removal is preffreable to other conventional technologies due to renewable energy and lower carbon emission, which is necessry for sustianable and clean environment.

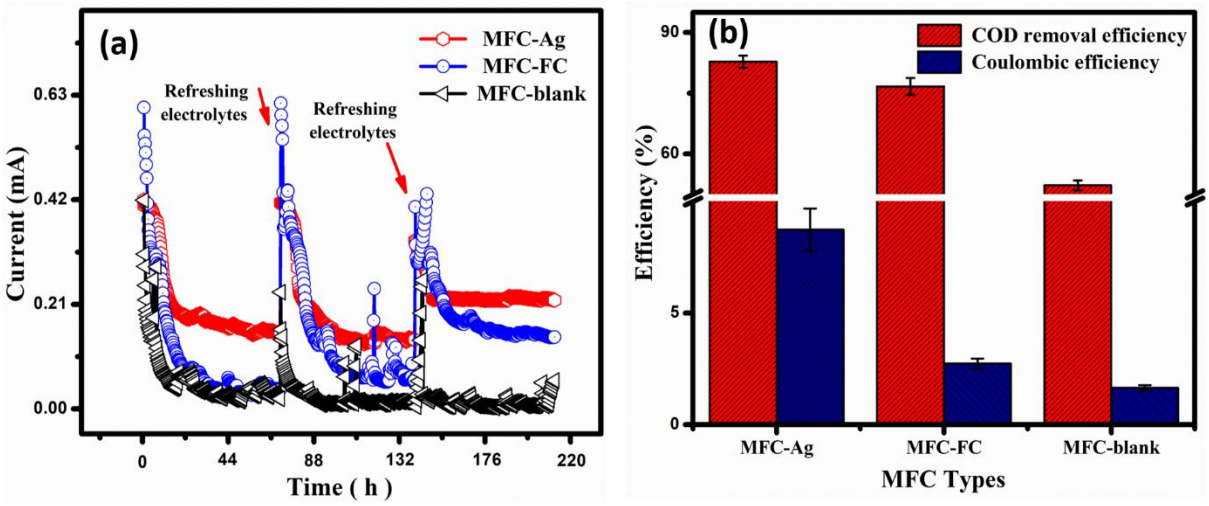

Fig. 5. Wastewater treatment efficiencies and electricity generation in MFCs (a) electrogenic performance and (b) treatment efficiencies of MFCs

The effect of various catholyte (silver) concentrations on electricity production, silver removal, and silver recovery efficiency was also evaluated. Five different concentrations of catholyte (i.e., 50, 100, 150, 250 and 500 mg/L) were used in respective MFCs, designated as MFC-50, MFC-100, MFC-150, MFC-250 and MFC-500, respectively. Fig. 6a shows the silver removal rate was increased with the concentration of silver in the catholyte. MFC-500 delivered highest silver removal (83 ± 0.7%) and recovery efficiency (67.8 ± 1.0%). Generally, a decreasing trend for COD removal, silver removal, and silver recovery was observed as MFC-500 < MFC-250 < MFC-150 < MFC-100 < MFC-50, suggesting that high concentration of silver in catholyte is favourable for treating the wastewater in MFCs. Moreover, voltage generation profile was also in accordance with the trend observed for silver removal at various concentrations (Fig. 6b). The low overpotential in MFC-500 as compared with other MFCs can also be attributed to the extra deposited AgNFs at the cathode surface, which may increase the conductivity and enhance the electron transfer kinetics by decreasing the charge transfer resistance (Fig. 6b). In situ, modified cathodes can be further utilized for various catalytic/

environmental applications, such as electrodeposited silver have been employed to improve the performance of air cathode MFC via mitigating the biofouling and catalyzing the ORR (Firouzjaei et al., 2018; Linge et al., 2018). This method will also bring back material to the production stream as a resource and will help to address the economic issues of electronic/semiconductor manufacturing industries. Thus, simultaneous waste removal and valorization can be achieved using this simple process, which does not rely on special lab facilities for implementation.

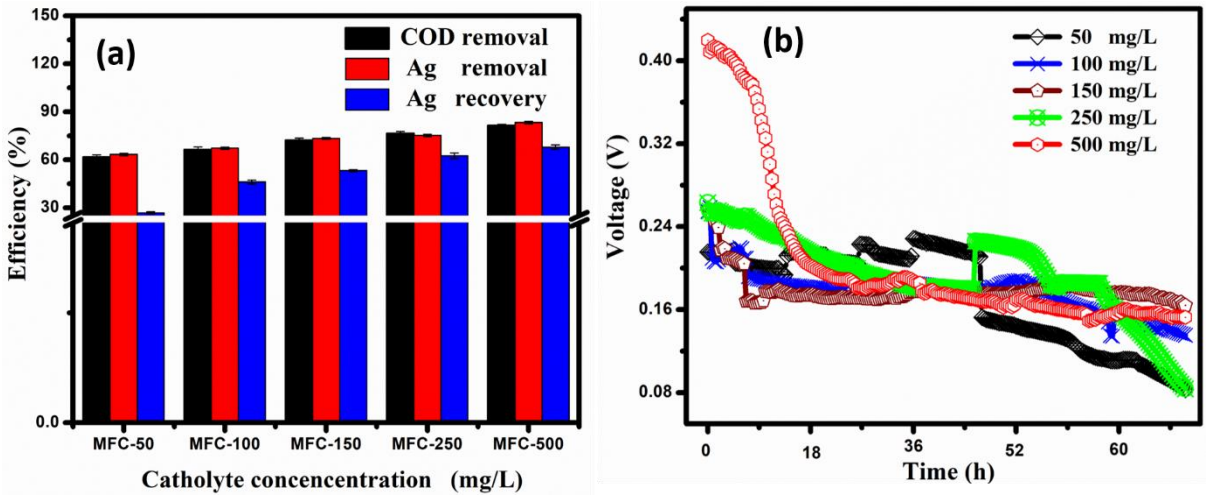

Fig. 6. Effect of various concentrations of catholyte on MFC performance (a) silver removal and silver recovery and COD removal efficiency (b) voltage generation profile

3.5. Characterization of the silver nanoflakes deposited on the cathode

Bioelectrochemical reduction of silver nitrate resulted in the deposition of silver nanoflakes (AgNFs) on the cathode surface. In order to investigate the morphology and nature of AgNFs several techniques such as XRD, SEM, XPS, EDX, XRF, and TEM were used. XRD pattern of the AgNFs revealed the characteristic peaks of the face-centered cubic structures of Ag at the 2θ = 38.12, 44.30, 64.42, 74.41 (JCPDS card No. 65-2871), which indicate the reduction

of the Ag+ ions to AgNFs by electrons produced *Pseudomonas aeruginosa* in the anode. Also, a short peak representing the graphite felt also appeared at the 2θ = 26.7 (Fig. 7). Interestingly, a high ratio of the plane (111) suggests that recovered AgNFs were dominated by (111) facets which is consistent with previous findings of the silver nanomaterials (Ali et al., 2017; Ali et al., 2016).

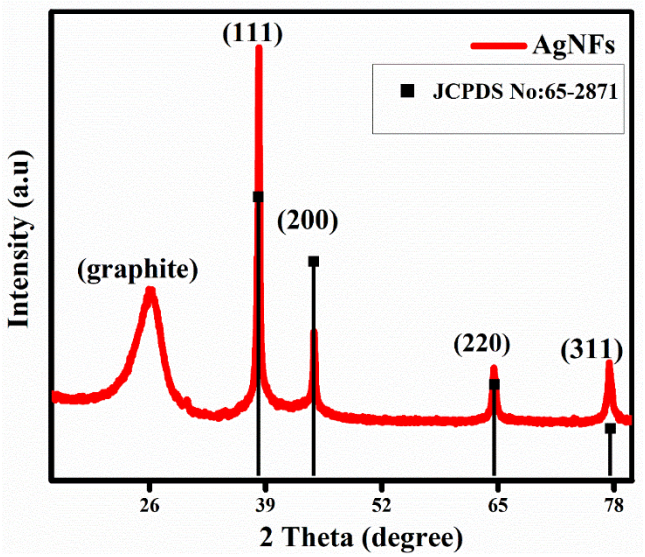

Fig. 7. XRD patterns of silver nanoflakes deposited on the cathode of MFC-Ag

The overall morphology of AgNFs indicated some irregularly shaped entities at higher magnification of SEM (Fig. 8 a, b). And Fig. 8 (c, d) shows the complete survey and Ag (3d) XPS spectrum of AgNFs. The overall survey of AgNFs recovered in MFC-Ag display the expected characteristic peaks of C1s, O1s at 285 and 574 and Ag (3d) (Fig. 8c). The Ag (3d) peaks were appeared as a doublet due to spin-orbit coupling ($3d_{5/2}$ and $3d_{3/2}$) at the binding energies of 368 eV and 374 eV respectively (Fig. 8d). These characteristic peaks at specific binding energies confirm the synthesis of AgNFs mediated by the electrochemical pathway in MFC-Ag (Ajitha et al., 2015; Yan et al., 2018). There were no oxide peaks in the XPS spectrum, indicating the high stability of AgNFs. However, carbon and oxygen peaks may arise

from the graphite felt fibres of cathode attached to AgNFs. Elemental composition analysis by Wavelength dispersive XRF of AgNFs showed recovered particles were 99 ± 0.05 % of pure silver (Fig. S2). The purity of the recovered AgNFs in this study was highest among the reported studies in literature (Choi and Cui, 2012; Ho, N. et al., 2017). All these results have highlighted the utility of the proposed method for extracting the silver from industrial wastewater even with low concentration.

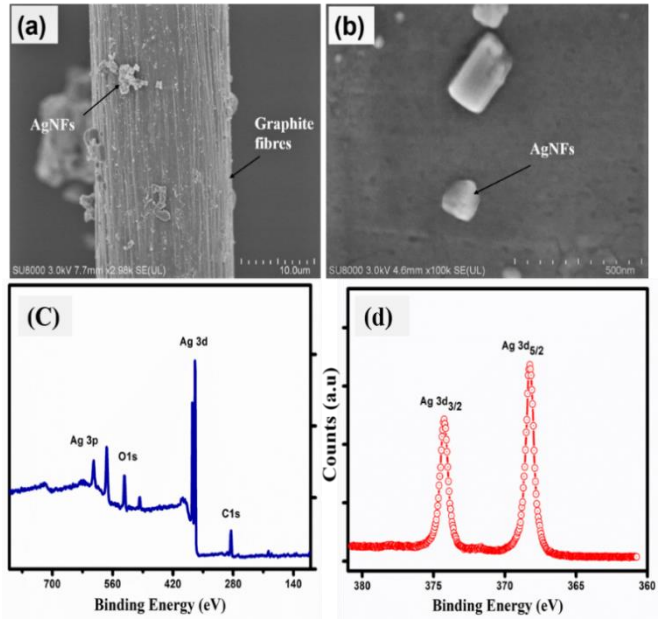

Fig. 8 SEM images of silver nanoflakes deposited on the cathode of MFC (a) AgNFs attached on graphite felt fibre, and (b) irregular shaped AgNFs at high magnification; The X-ray photoelectron spectrum (XPS) of AgNFs (c) the overall survey and (d) the spectrum of Ag (3d)

A more detailed understanding of the morphology of AgNFs was provided by high-resolution TEM (HRTEM) images. HRTEM images at various magnifications, and selected area electron diffraction (SAED) pattern are displayed in Fig. 9. The variable size range (10-26 nm) and the period of 2d = 0.205 nm in AgNFs lattice were evident in Fig. 9c. Also, the indexed SAED pattern with bright and circular fringes corresponding to the (111), (200), (220)

and (311) planes of crystalline AgNFs (Fig. 9d). Current findings are in accordance with our XRD results and previous studies about AgNFs (Wei et al., 2015). These results explain the successful bioelectrochemical reduction of silver ions to AgNFs and subsequent electrodeposition at the cathode. The proposed underlying mechanism for the synthesis of AgNFs can be two steps, (a) electron provided from the anode transform the Ag^{+} to Ag^{0} at the cathode surface, (b) which initiate the nucleation and growth of nanoflakes (Ali et al., 2019). Hence, the current method delivers in situ waste remediation approach for industrial wastewater and also provide an opportunity for waste recycling (valorization). This one-step conversion of waste to wealth will defiantly address challenges required for sustainable waste management.

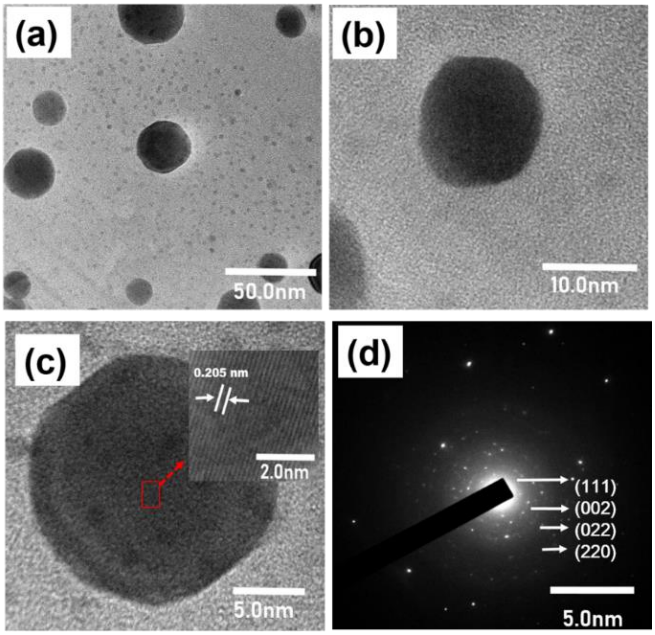

Fig. 9. TEM images of silver nanoflakes (AgNFs) under various resolutions (a) & (b) displaying the spherical shaped AgNFs (C) HRTEM image of AgNFs (d) SAED pattern of AgNFs

3.6. Anti-biofouling activity

3.6.1. Antibacterial sensitivity test

The antibacterial activity of the AgNFs against the *E.coli*, *Shewanella*, and *Pseudomonas aeruginosa* was observed by the modified disk diffusion method (Fig. 10). The control graphite felt didn't show any inhibition zone in all cases, while Ag-electrode clearly showed the inhibition zones of 13.8 ± 0.12 mm, 15 ± 0.24 mm and 10.45 ± 4 mm for *E.coli*, *Shewanella* and *Pseudomonas aerogenosa* respectively. A positive correlation (R^2 =0.93) was observed between anti-biofouling potential and concentration of recovered AgNFs (Fig. S3). These results indicate the effectiveness of electrochemically deposited AgNFs as an inexpensive anti-biofouling agent. Thus, recovered AgNFs could be directly applied for biofouling mitigation in electrochemical reactors, where low dissolved oxygen renders the slow reaction kinetics due to mass transfer losses. Our findings will advance the strategies used for biofilm inhibition and improving the catalytic performance of fuel cells (Noori et al., 2016).

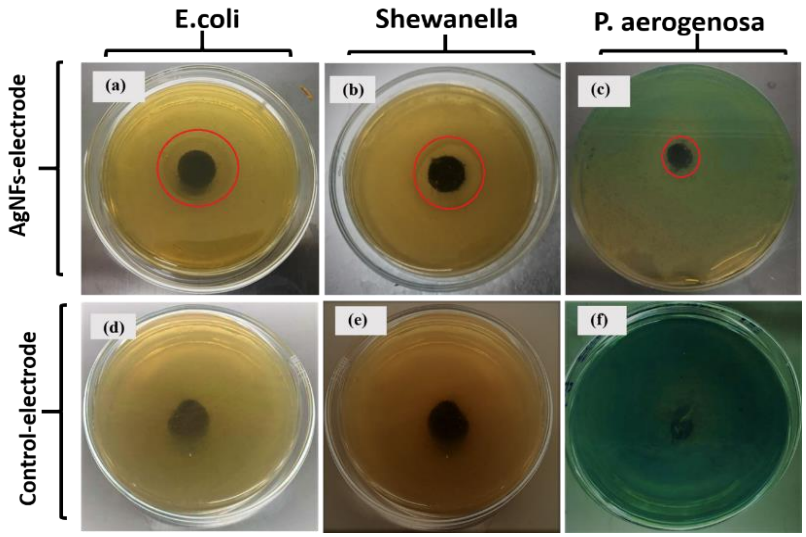

Fig. 10. Antibacterial activities of electrochemically deposited AgNFs, (a, b & c) indicate the inhibition zones formation with Ag-electrode by *E.coli*, *Shewanella* and *Pseudomonas aeruginosa*, respectively, (d, e, f) represent the no growth inhibition with control electrodes

3.6.2. Activated sludge immersion test

The anti-biofouling activity of the silver deposited electrodes (Ag-electrode) is also compared with control a non-silver control (graphite) after seven days incubation in activated sludge. CLSM micrographs stained by PI and DAPI shows the majority of dead bacterial cells which indicate the biofilm formation was inhibited on Ag-electrode (Fig. 11a, b) due to the antibacterial effect of AgNFs. Whereas, biofilm formation was evident from the extensive bacterial growth and presence of EPS matrix on control electrodes (Fig.11d, e). The additional evidence provided by the SEM micrographs also indicated the biofilm formation and dense EPS matrix on the control electrode (Fig.11c, f). However, few bacteria and absence of EPS matrix on Ag-electrode reveals its anti-biofouling activity, and these findings also support the CLSM results. Earlier, EPS production has been entirely attributed to adhesion and successful establishment of biofouling in membrane reactors (Kim, T.-S. et al., 2019; Yi et al., 2019). Moreover, EPS has been postulated to contribute most to the hydraulic resistance of biofilms. Biofouling in ORR based reactors increase the mass transport losses and lower their optimal performance by consuming the DO (Huang, J. et al., 2019; Kim, H.-S. et al., 2019). Interestingly, Ag-based catalytic materials have been regarded as an efficient platinum free electrocatalysts toward ORR for anion exchange membrane fuel cells (Erikson et al., 2019; Kim, T.-S. et al., 2019).

Electrodes with innate anti-biofouling potential and enhanced catalytic properties are required for the long-term and stable performance of fuel cells and biological reactors. Therefore, it is expected Ag-electrode has potential applications for anti-biofouling and ORR processes, that will not only mitigate the biofouling problem but will also enhance the catalytic reduction of oxygen (Farhat et al., 2019; Noori et al., 2018). Briefly, in situ preparation of antibiofouling material was achieved from wastewater, which will reduce the cost of antibiofouling materials for sustainable resource recovery or waste valorization.

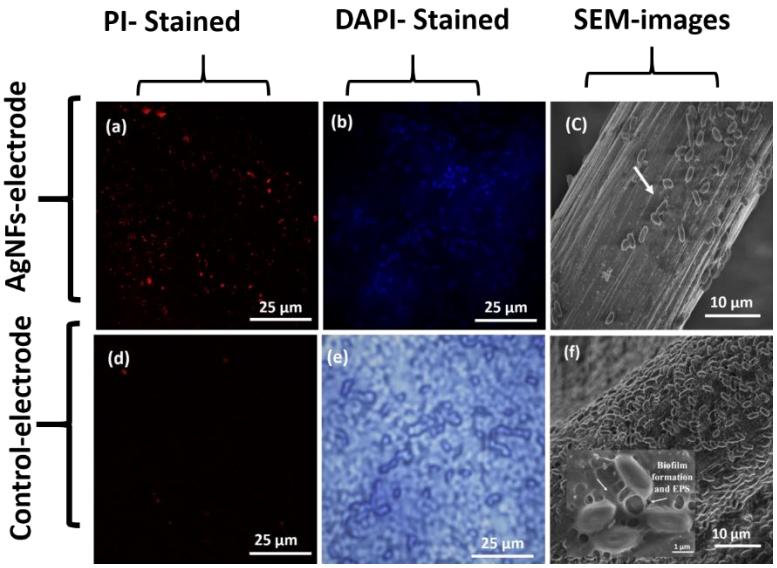

Fig. 11. CLSM and SEM results of activated sludge immersion test, images (a, d), (b, e) and (c, f) represent the PI-stained, DAPI stained and SEM images respectively. Images a, b, and c specified the biofilm inhibition at Ag-electrode and images e and f show the biofilm formation at the control electrode

4. Conclusion

Silver contaminated wastewater can serve as a cost-effective catholyte for MFCs. The current method can recover approximately 339 g of silver from 1.5 litre of wastewater after 30 days. Therefore, stacked MFCs with high retention volumes can efficiently treat industrial wastewater. The eco-friendly method has not only recovered unprecedented amounts of silver (67.8%) but also generated sufficient bioenergy (3006 mW/m^3) from low concentrated wastewater (500 mg/L) through MFC. The lowest solution resistance (24.38 Ω) and charge transfer resistance (5.413 Ω) of MFC-Ag improved the reaction kinetics to deliver a significant exchange current density (0.086 Acm^{-2}) in the reactor. Highest COD removal efficiency of MFC-Ag (82.7 ± 1.5%) compared with controls was also linked with the enhanced silver removal efficiency (83 ± 0.7%). High crystalline and pure (99 %) silver was recovered from silver containing wastewater. The high potential of recovered silver in anti-biofouling applications has showed a way forward in exploring the utility of recovered nanoflakes

particularly in membrane bioreactors. The one-step resource recovery and valorization of silver from industrial wastewater can contribute significantly in moving towrads circular economy. In contrast to conventional technologies, high efficiency and effective resource management indicate the high potential of this clean process for attaining environemntal protection and economic sustainability. It implies that, current findings will minimize the continously increasing gap between production and useage of silver. The present study was conducted on pilot scale, therefore large scale applications for real wastewater must be evaluated. Implications of current study may involve high capital cost and duarabaility of electrode materials for longterm industrial applications. Operational issues associated with optimum recovery efficiency, types of wastewater and anodic biofilm development must also be considered. In addition, stability of generataed electricty by industrial wastewater and suitable power management programs can be useful for attaining the sustianable goals. Futrustritc applications of recovered silver nanoflakes can replace the platinum based precious catalysts, which is consdiered as a major challenege for renewable energy conversion systems.

Acknowledgments

This work was supported by the National Key R&D Program of China (2017YFA0207203), Science and Technology Service Network Initiative (KFJ-STS-ZDTP-048), the Key Research and Development Program of Ningxia (2017BY064), National Natural Science Foundation of China (21407160) and Strategic Priority Research Program of the Chinese Academy of Sciences (XDA09030203).

Thanks for the University of Chinese Academy of Sciences (UCAS) Scholarship for International Students (to Jafar Ali).

Conflicts of Interest: The authors declare no conflict of interests.

References

Ajitha, B., Reddy, Y.A.K., Reddy, P.S., 2015. Green synthesis and characterization of silver nanoparticles using Lantana camara leaf extract. Materials Science and Engineering: C 49, 373-381.
Ali, J., Ali, N., Jamil, S.U.U., Waseem, H., Khan, K., Pan, G., 2017. Insight into eco-friendly fabrication of silver nanoparticles by Pseudomonas aeruginosa and its potential impacts. Journal of Environmental Chemical Engineering 5(4), 3266-3272.
Ali, J., Ali, N., Wang, L., Waseem, H., Pan, G., 2019. Revisiting the mechanistic pathways for bacterial mediated synthesis of noble metal nanoparticles. J. Microbiol. Methods 159, 18-25.
Ali, J., Hameed, A., Ahmed, S., Ali, M.I., Zainab, S., Ali, N., 2016. Role of catalytic protein and stabilising agents in the transformation of Ag ions to nanoparticles by Pseudomonas aeruginosa. IET nanobiotechnology 10(5), 295-300.
Ali, J., Sohail, A., Wang, L., Haider, M.R., Mulk, S., Pan, G., 2018. Electro-Microbiology as a Promising Approach Towards Renewable Energy and Environmental Sustainability. Energies 11(7), 1-30.
Cheng, S., Liu, H., Logan, B.E., 2006. Increased power generation in a continuous flow MFC with advective flow through the porous anode and reduced electrode spacing. Environ. Sci. Technol. 40(7), 2426-2432.
Choi, C., Cui, Y., 2012. Recovery of silver from wastewater coupled with power generation using a microbial fuel cell. Bioresour. Technol. 107, 522-525.
Deycard, V.N., Schäfer, J., Petit, J.C., Coynel, A., Lanceleur, L., Dutruch, L., Bossy, C., Ventura, A., Blanc, G., 2017. Inputs, dynamics and potential impacts of silver (Ag) from urban wastewater to a highly turbid estuary (SW France). Chemosphere 167, 501-511.
Djellabi, R., Yang, B., Sharif, H.M.A., Zhang, J., Ali, J., Zhao, X., 2019. Sustainable and easy recoverable magnetic TiO2-Lignocellulosic Biomass@ Fe3O4 for solar photocatalytic water remediation. J.Clean.Prod. 233, 841e847.
Dutta, A., 2019. Impact of silver price uncertainty on solar energy firms. J.Clean.Prod. 225, 1044-1051.
Erikson, H., Sarapuu, A., Tammeveski, K., 2019. Oxygen Reduction Reaction on Silver Catalysts in Alkaline Media: a Minireview. ChemElectroChem 6(1), 73-86.
Farhat, N., Javier, L., Van Loosdrecht, M., Kruithof, J., Vrouwenvelder, J.S., 2019. Role of feed water biodegradable substrate concentration on biofouling: Biofilm characteristics, membrane performance and cleanability. Water Res. 150, 1-11.
Feng, C., Ma, L., Li, F., Mai, H., Lang, X., Fan, S., 2010. A polypyrrole/anthraquinone-2, 6-disulphonic disodium salt (PPy/AQDS)-modified anode to improve performance of microbial fuel cells. Biosens. Bioelectron. 25(6), 1516-1520.
Firouzjaei, M.D., Shamsabadi, A.A., Aktij, S.A., Seyedpour, S.F., Sharifian Gh, M., Rahimpour, A., Esfahani, M.R., Ulbricht, M., Soroush, M., 2018. Exploiting Synergetic Effects of Graphene Oxide and a Silver-Based Metal–Organic Framework To Enhance Antifouling and Anti-Biofouling Properties of Thin-Film Nanocomposite Membranes. ACS applied materials & interfaces 10(49), 42967-42978.
Grandell, L., Thorenz, A., 2014. Silver supply risk analysis for the solar sector. Renewable energy 69, 157-165.
Greulich, C., Braun, D., Peetsch, A., Diendorf, J., Siebers, B., Epple, M., Köller, M., 2012. The toxic effect of silver ions and silver nanoparticles towards bacteria and human cells occurs in the same concentration range. Rsc Advances 2(17), 6981-6987.
Grobbler, C., Virdis, B., Nouwens, A., Harnisch, F., Rabaey, K., Bond, P.L., 2018. Effect of the anode potential on the physiology and proteome of Shewanella oneidensis MR-1. Bioelectrochemistry 119, 172-179.
Heijne, A.T., Liu, F., Weijden, R.v.d., Weijma, J., Buisman, C.J., Hamelers, H.V., 2010. Copper recovery combined with electricity production in a microbial fuel cell. Environ. Sci. Technol. 44(11), 4376-4381.
Ho, N., Babel, S., Kurisu, F., 2017. Bio-electrochemical reactors using AMI-7001S and CMI-7000S membranes as separators for silver recovery and power generation. Bioresour. Technol. 244, 1006-1014.

Ho, N., Babel, S., Sombatmankhong, K., 2018. Bio-electrochemical system for recovery of silver coupled with power generation and wastewater treatment from silver (I) diammine complex. Journal of Water Process Engineering 23, 186-194.
Ho, N.A.D., Babel, S., Sombatmankhong, K., 2017. Factors influencing silver recovery and power generation in bio-electrochemical reactors. Environmental Science and Pollution Research 24(26), 21024-21037.
Huang, J., Gu, Y., Zeng, G., Yang, Y., Ouyang, Y., Shi, L., Shi, Y., Yi, K., 2019. Control of indigenous quorum quenching bacteria on membrane biofouling in a short-period MBR. Bioresour. Technol. 283, 261.
Huang, T., Song, D., Liu, L., Zhang, S., 2019. Cobalt recovery from the stripping solution of spent lithium-ion battery by a three-dimensional microbial fuel cell. Sep. Purif. Technol. 215, 51-61.
Islam, M.A., Ethiraj, B., Cheng, C.K., Yousuf, A., Khan, M.M.R., 2017. Electrogenic and Antimethanogenic Properties of Bacillus cereus for Enhanced Power Generation in Anaerobic Sludge-Driven Microbial Fuel Cells. Energy Fuels 31(6), 6132-6139.
Kahlon, S.K., Sharma, G., Julka, J., Kumar, A., Sharma, S., Stadler, F.J., 2018. Impact of heavy metals and nanoparticles on aquatic biota. Environ. Chem. Lett. 16(3), 919-946.
Kim, B., Chang, I.S., 2018. Elimination of voltage reversal in multiple membrane electrode assembly installed microbial fuel cells (mMEA-MFCs) stacking system by resistor control. Bioresour. Technol. 262, 338-341.
Kim, H.-S., Lee, J.Y., Ham, S.-Y., Lee, J.H., Park, J.-H., Park, H.-D., 2019. Effect of biofilm inhibitor on biofouling resistance in RO processes. Fuel 253, 823-832.
Kim, T.-S., Park, S.-H., Park, D., Lee, J.-H., Kang, S., 2019. Surface immobilization of chlorhexidine on a reverse osmosis membrane for in-situ biofouling control. J. Membr. Sci. 576, 17-25.
Koseoglu, H., Kitis, M., 2009. The recovery of silver from mining wastewaters using hybrid cyanidation and high-pressure membrane process. Miner. Eng. 22(5), 440-444.
Lei, C., Yan, B., Chen, T., Wang, X.-L., Xiao, X.-M., 2018. Silver leaching and recovery of valuable metals from magnetic tailings using chloride leaching. J.Clean.Prod. 181, 408-415.
Linge, J.M., Erikson, H., Kozlova, J., Sammelselg, V., Tammeveski, K., 2018. Oxygen reduction reaction on electrochemically deposited silver nanoparticles from non-aqueous solution. J. Electroanal. Chem. 810, 129-134.
Liu, H., Cheng, S., Logan, B.E., 2005. Production of electricity from acetate or butyrate using a single-chamber microbial fuel cell. Environ. Sci. Technol. 39(2), 658-662.
Nancharaiah, Y., Mohan, S.V., Lens, P., 2016. Biological and bioelectrochemical recovery of critical and scarce metals. Trends Biotechnol. 34(2), 137-155.
Nimje, V.R., Chen, C.-Y., Chen, H.-R., Chen, C.-C., Huang, Y.M., Tseng, M.-J., Cheng, K.-C., Chang, Y.-F., 2012. Comparative bioelectricity production from various wastewaters in microbial fuel cells using mixed cultures and a pure strain of Shewanella oneidensis. Bioresour. Technol. 104, 315-323.
Niu, B., Chen, Z., Xu, Z., 2017. An integrated and environmental-friendly technology for recovering valuable materials from waste tantalum capacitors. J.Clean.Prod. 166, 512-518.
Noori, M.T., Jain, S.C., Ghangrekar, M., Mukherjee, C., 2016. Biofouling inhibition and enhancing performance of microbial fuel cell using silver nano-particles as fungicide and cathode catalyst. Bioresour. Technol. 220, 183-189.
Noori, M.T., Tiwari, B., Mukherjee, C., Ghangrekar, M., 2018. Enhancing the performance of microbial fuel cell using AgPt bimetallic alloy as cathode catalyst and anti-biofouling agent. Int. J. Hydrogen Energy 43(42), 19650-19660.
Raghavulu, S.V., Babu, P.S., Goud, R.K., Subhash, G.V., Srikanth, S., Mohan, S.V., 2012. Bioaugmentation of an electrochemically active strain to enhance the electron discharge of mixed culture: process evaluation through electro-kinetic analysis. RSC Advances 2(2), 677-688.
Rigoldi, A., Trogu, E.F., Marcheselli, G.C., Artizzu, F., Picone, N., Colledani, M., Deplano, P., Serpe, A., 2018. Advances in Recovering Noble Metals from Waste Printed Circuit Boards (WPCBs). ACS Sustainable Chemistry & Engineering 7(1), 1308-1317.

Saunders, S.H., Newman, D.K., 2018. Extracellular Electron Transfer Transcends Microbe-Mineral Interactions. Cell Host Microbe 24(5), 611-613.
Sravan, J.S., Butti, S.K., Verma, A., Mohan, S.V., 2017. Phasic availability of terminal electron acceptor on oxygen reduction reaction in microbial fuel cell. Bioresour. Technol. 242, 101-108.
Srikanth, S., Mohan, S.V., 2012. Influence of terminal electron acceptor availability to the anodic oxidation on the electrogenic activity of microbial fuel cell (MFC). Bioresour. Technol. 123, 480-487.
Staroń, P., Chwastowski, J., Banach, M., 2017. Sorption and desorption studies on silver ions from aqueous solution by coconut fiber. J.Clean.Prod. 149, 290-301.
Syed, S., 2016. Silver recovery aqueous techniques from diverse sources: Hydrometallurgy in recycling. Waste Manage. (Oxford) 50, 234-256.
Wang, Y.-H., Wang, B.-S., Pan, B., Chen, Q.-Y., Yan, W., 2013. Electricity production from a bio-electrochemical cell for silver recovery in alkaline media. Applied energy 112, 1337-1341.
Ward, C., Pan, J., Colman, B., Wang, Z., Gwin, C., Williams, T., Ardis, A., Gunsch, C., Hunt, D., 2019. Conserved Microbial Toxicity Responses for Acute and Chronic Silver Nanoparticle Treatments in Wetland Mesocosms. Environ. Sci. Technol. 53(6), 3268.
Wei, L., Lu, J., Xu, H., Patel, A., Chen, Z.-S., Chen, G., 2015. Silver nanoparticles: synthesis, properties, and therapeutic applications. Drug Discovery Today 20(5), 595-601.
Yan, Z., Fu, L., Zuo, X., Yang, H., 2018. Green assembly of stable and uniform silver nanoparticles on 2D silica nanosheets for catalytic reduction of 4-nitrophenol. Applied Catalysis B: Environmental 226, 23-30.
Yang, E., Alayande, A.B., Kim, C.-M., Song, J.-h., Kim, I.S., 2018. Laminar reduced graphene oxide membrane modified with silver nanoparticle-polydopamine for water/ion separation and biofouling resistance enhancement. Desalination 426, 21-31.
Yi, M., Lau, C., Xiong, S., Wei, W., Liao, R., Shen, L., Lu, A., Wang, Y., 2019. Zwitterion-Ag Complexes That Simultaneously Enhance Biofouling Resistance and Silver Binding Capability of Thin Film Composite Membranes. ACS applied materials & interfaces 11(17), 15698.
Yong, X.-Y., Feng, J., Chen, Y.-L., Shi, D.-Y., Xu, Y.-S., Zhou, J., Wang, S.-Y., Xu, L., Yong, Y.-C., Sun, Y.-M., 2014. Enhancement of bioelectricity generation by cofactor manipulation in microbial fuel cell. Biosens. Bioelectron. 56, 19-25.
Zhang, H.-M., Fan, Z., Xu, W., Feng, X., Wu, Z.-C., 2017. Retrieval of Au, Ag, Cu precious metals coupled with electric energy production via an unconventional coupled redox fuel cell reactor. J. Hazard. Mater. 338, 194-201.
Zhang, P., Liu, J., Qu, Y., Feng, Y., 2017. Enhanced Shewanella oneidensis MR-1 anode performance by adding fumarate in microbial fuel cell. Chem. Eng. J. 328, 697-702.
Zhang, X., He, W., Ren, L., Stager, J., Evans, P.J., Logan, B.E., 2015. COD removal characteristics in air-cathode microbial fuel cells. Bioresour. Technol. 176, 23-31.
Zhao, L., Deng, J., Hou, H., Li, J., Yang, Y., 2019. Investigation of PAH and oil degradation along with electricity generation in soil using an enhanced plant-microbial fuel cell. J.Clean.Prod. 221, 678-683.